

Acceleration Factors for Combined-Accelerated Stress Testing of Photovoltaic Modules

Peter Hacke,* Michael Owen-Bellini, Michael D. Kempe, Dana B. Sulas-Kern, David C. Miller, Marko Jankovec, Stefan Mitterhofer, Marko Topič, Sergiu Spataru, William Gambogi, and Tadanori Tanahashi

Combined-accelerated stress testing (C-AST) is developed to establish the durability of photovoltaic (PV) products, including for degradation modes that are not a priori known or examined in standardized tests. C-AST aims to comprehensively represent the sample, stress factors, and their combinations using levels at the statistical tails of the natural environment. Acceleration factors for relevant climate sequences within the C-AST cycle with respect to the Florida USA climate are estimated for selected degradation mechanisms. It is found that for degradation of the outer backsheet polymer layer, the acceleration factor of the tropical climate sequence (the longest of the climate sequences) is $f(T, G) = 17.3$ with ultraviolet photodegradation; for polyethylene terephthalate hydrolysis (backsheets), $f(T, RH) = 426$; for electrochemical corrosion (PV cell), $f(I) = 14.1$; and for PbSn solder fatigue $f(\Delta T, r(T)) = 17.3$. Here, T is the module temperature, G is the broadband spectrum irradiance on the plane of array of the module, RH is the relative humidity on the module surface, I is the leakage current through the module packaging, and $r(T)$, the number of temperature reversals. The methods discussed herein are generally applicable for evaluating acceleration factors in other accelerated test methods.

trouble in the field. For example, technical papers emerged in 1977 that showed PV module susceptibility to system voltage in humid conditions, presently referred to as potential-induced degradation (PID).^[1,2] Methods for PID testing were proposed in 1978 but not widely implemented.^[3] While some work continued in thin film technology,^[4] the phenomenon was largely ignored until field failures with various PID types were extensively reported. The PID issue led to a great deal of financial cost in the 2005 to 2015 time-frame.^[5,6] Field-relevant PID test methods were agreed upon and standardized in IEC 62 804–1 in 2015^[7] and incorporated into IEC 61 215 qualification testing in 2021,^[8] which is 44 years after the first publications about PID. Faulty products were produced, shipped, and sold with many consumers unaware of the issue. Other examples of degradation modes discovered after extensive shipments of PV modules include light and elevated temperature induced degradation

1. Introduction


Numerous field failures are observed in photovoltaic (PV) modules that pass standardized design qualification and type approval testing. Standardized tests are typically mechanism-specific and only developed after the failure mode has caused extensive

(LETID), an important degradation mode in modules with passivated emitter and rear contact (PERC) cells,^[9–11] and cracking of polyamide (PA) and certain polyvinylidene fluoride (PVDF)-based backsheets.^[12,13]

With the discovery of new degradation or failure mechanisms, numerous tests were added to comprehensively examine these

P. Hacke, M. Owen-Bellini, M. D. Kempe, D. B. Sulas-Kern, D. C. Miller
Reliability and System Performance
National Renewable Energy Laboratory
Golden, CO 80401, USA
E-mail: peter.hacke@nrel.gov

M. Jankovec, S. Mitterhofer, M. Topič
Faculty of Engineering
University of Ljubljana
1000 Ljubljana, Slovenia

 The ORCID identification number(s) for the author(s) of this article can be found under <https://doi.org/10.1002/solr.202300068>.

© 2023 The Authors. Solar RRL published by Wiley-VCH GmbH. This is an open access article under the terms of the Creative Commons Attribution License, which permits use, distribution and reproduction in any medium, provided the original work is properly cited.

DOI: 10.1002/solr.202300068

S. Spataru
Department of Electrical and Photonics Engineering
Technical University of Denmark
4000 Roskilde, Denmark

W. Gambogi
Photovoltaics and Advanced Materials
DuPont Central Research and Development
Wilmington, DE 19803, USA

T. Tanahashi
Renewable Energy Research Center
National Institute of Advanced Industrial Science and Technology (AIST)
Koriyama 963-0298, Japan

failure modes, making industry standards increasingly complex. For example, the 2005 edition of IEC 61 215, “Crystalline silicon terrestrial photovoltaic (PV) modules – Design qualification and type approval” international standard contains 18 test procedures,^[14] whereas the 2021 edition contains 22 module quality test procedures.^[15] Following the creation of failure mechanism, or mode-specific tests, additional and longer test sequences based on these are invariably implemented to more extensively evaluate durability^[16] and aid in insurance pricing.^[17]

Combined-accelerated stress testing (C-AST) was introduced to evaluate PV module durability and more comprehensively discover additional failure modes.^[18] C-AST has been extended to other balance of systems (BOS) components including PV connectors.^[19] The purpose of C-AST is to evaluate both known failure modes and those for which mechanism-specific tests have not been created. This is accomplished by stressing representative samples and achieving accelerated degradation by applying multiple simultaneous stress factors at combinations and levels derived from the statistical tails of the PV application in the natural environment over the major climates, as well as including diurnal stress sequences such as freeze/thaw cycles. C-AST is intended to quantify and reduce residual risk. This may include risk when adopting new designs/materials, the risk from incremental changes including using thinner cells or reduced metallization for cost savings, and risks from the failure of critical parts like an edge seal for moisture-sensitive PV cells which may exhibit problems if a manufacturing process changes.^[17] So far, C-AST has been used for duplicating field failures in failure-susceptible polyamide and polyvinylidene fluoride-based backsheets,^[20] potential-induced degradation,^[21] light-induced degradation,^[21] connector failures,^[22] and poor junction box connections.^[23] The C-AST protocol, which is agnostic to the material or design being tested, is designed to objectively analyze product durability. Considering the significant (US \$151 billion) international PV industry,^[24] the present addressable risks as well as the benefits of progress in reducing risks are substantial.

The extent of acceleration that is achieved with C-AST has not yet been clarified and is different for every mode and PV system location. Here, we estimate how long one should test a product in C-AST for the goal of relating the test and observed degradation to the number of years in the field to achieve the same extent of degradation for various degradation modes. We do this by estimating the acceleration factors for various mechanisms, such as ultraviolet (UV)-induced photodegradation of the outer polymer layer (backsheets), hydrolysis of polyethylene terephthalate (PET) that is used for the electrical insulation in many backsheet types, cell electrochemical corrosion based on charge transfer through the module packaging, Sn/Pb solder fatigue due to temperature cycling, and degradation through cyclic loading such as from windstorms.

2. Background

An acceleration factor is the ratio of the degradation or failure rate during accelerated aging to that of field use. For example, in the case of acceleration by temperature

$$AF = \frac{R_{T_1}}{R_{T_2}} \quad (1)$$

where R_{T_1} is the rate at test temperature T_1 at which the accelerated test is being performed, R_{T_2} is the rate at the use temperature T_2 . If temperature and other conditions acting as independent variables causing the degradation or failure such as irradiance (G) and relative humidity (RH), are also varying during the period, the rate is considered as

$$R = \frac{1}{N} \sum^N R(T, G, RH) \quad (2)$$

where rate over the whole period is the average of individual rates with number segments of equal length N .

Some studies of acceleration factors for degradation of PV modules and their components exist in the literature. As background, theory-based analytical equations that are used here are reviewed. Koehl et al. and Kimball et al. separately examined the acceleration of the 85 °C 85% testing condition in the dark over the use environment.^[25,26] Methodologies, review, and examples for computing the degradation of PV module materials are given by Kempe et al.^[27] These authors gave a degradation rate proportionality formula for PET, as measured by degradation in mechanical properties such as embrittlement, elongation to break, and rate to failure (reciprocal of time to failure), as

$$R(T, RH) \propto e^{-\frac{E_a}{kT}} RH^n \quad (3)$$

PET material serving as a structural and electrical insulating layer for many backsheet types has been well studied such that the activation energy E_a and exponential factor for relative humidity n have been determined to be $129 \pm 6.7 \text{ kJ mol}^{-1}$ and 2, respectively.^[27–29] The UV component that can cause the degradation of PET is neglected here because a properly made backsheet will typically contain UV absorbers or additional protective outer layers that prevent damaging UV irradiation from reaching the PET layer.

Examination of the acceleration with irradiation and temperature on the surfaces of backsheets was studied by Koehl et al.,^[30] on polymeric front sheets by Kempe et al.,^[31] and in a comprehensive empirical study of various polymers by Fischer and Ketola.^[32] The degradation rate is given as

$$R(T, G) \propto G^x \cdot e^{-\frac{E_a}{kT}} \quad (4)$$

where E_a is $38.5 \pm 21.6 \text{ kJ mol}^{-1}$ and x (the reciprocity coefficient) is 0.5 ± 0.21 . The study also considered degradation in aggregate of material parameters of yellowness index, UV cut-on, UV-transmittance, and solar photon quantum efficiency-weighted transmittance.^[30–32] Humidity may or may not have an important effect on degradation rate and is highly dependent on the kinetics of a given degradation pathway. On average, humid environment (Miami, Florida) increases degradation rate by about 12% over the dry environment (Phoenix, Arizona) in a survey of 50 polymer or polymer matrices (e.g., for cracking of paints and coatings).^[32] We do not have enough data for degradation of any one specific PV outer polymer layer. Anticipating

the average effect of humidity is relatively small or could even slow down the degradation, the humidity effect is not included in the acceleration with irradiation and temperature on the outer surfaces of a backsheet.

Hacke et al. tested modules in humidity under system voltages examining the leakage current from modules in Florida.^[33] If the rate of corrosion damage is assumed to be a function of total coulombs transferred per perimeter length of module as proposed by Mon et al.,^[34,35] then the rate of damage to the cells is proportional to $\int_t I \cdot dt$, the current transferred over the time duration, for a given voltage level in the cell circuit.

Module degradation due to thermal cycling may be calculated using the equation developed by Bosco et al. for PbSn solder bonds in conventional glass/backsheet modules with polyethylene-co-vinyl acetate (EVA) encapsulant^[36] based on the well-established Coffin–Manson and Norris–Landzberg models and the calculated accumulation of inelastic strain energy (damage) within the solder joint. The damage from specified weather inputs is given as

$$D = C \cdot \Delta T^n \cdot r(T)^b e^{\frac{-Q}{RT_{\max}}} \quad (5)$$

where $C = 239.9$ Pa, $n = 1.9$, $b = 0.33$, $Q = 11.58$ kJ mol⁻¹, and ΔT is the mean daily maximum cell temperature change. The temperature reversal term, $r(T)$, is the number of times the temperature history increases or decreases across the reversal temperature, T , over the course of a year.

Acceleration in mechanical loading needs more study to give definitive acceleration factors. However, some studies show typical frequencies of module oscillations are in the range of 10–35 Hz.^[37] Assuming a 24 h wind storm, e.g., a tropical storm in Florida,^[38] with a 14 Hz resonance frequency that we measured,^[39] about 1 209 600 cycles per day would result. The pressure developed on the module varies with wind speed and mounting, but 39.3 m s⁻¹ has been reported to result in a dynamic pressure of 1000 Pa^[40]; however, these authors found that similar pressure could occur in a nonuniform manner at wind speeds of 20.7 m s⁻¹.

3. Experimental Section

The C-AST equipment consists of a weathering chamber with four 6500 W Xenon lamps (consistent with ASTM D7869^[41] and including CIRA infrared filters) used to apply up to 0.95 W m⁻² nm⁻¹ at 340 nm (1.9 suns, relative to the AM1.5 G spectrum in IEC 60 904-3) full spectrum light on the faces of six mini-modules connected to adjustable resistive loads and 7.5% ($\pm 2.5\%$) albedo on the rear achieved with aluminum reflectors. Temperature and humidity controls in the chamber along with the heating from the lamps produced module temperatures between -40 and 90 °C, with relative humidity between 2% and 100%. System voltage up to 1200 V could be applied to the cell circuit with power supplies (one each for + and - polarity). The resulting leakage current was measured on the voltage supply side and aluminum foil tape was placed on the module perimeter connected to the ground. For results presented in this work, modules were subject to -600 V system voltage exclusively during periods of illumination. The system for measuring leakage current

from modules in the field has been previously published^[42] and was implemented here. Mechanical pressure was applied with pneumatic pistons. Further information about the equipment can be seen in previous publications.^[18,20,21]

The C-AST protocol was first introduced with the “Tropical” climate test sequence based on ASTM D7869 standard with PV-specific modifications including the addition of system voltage and mechanical pressure as experienced by fielded modules.^[18] When evaluating PVDF-based backsheets, it was hypothesized and later confirmed that the Tropical cycle maintains humidity levels producing a plasticizing (softening) effect such that cracks did not form. Therefore, it was necessary to introduce additional test sequences including those representing dry climates. Introducing such additional climate sequences with low relative humidity resulted in backsheet PVDF films that became harder with a higher modulus of elasticity^[43] and cracking similar to that seen in field specimens.^[20,44]

C-AST implements stress levels and combinations consistent with those in the natural environment, to minimize the occurrence of false positive and false negative failures. A graphical illustration of the protocol used in this testing is shown in **Figure 1**. Detailed line-by-line recipes developed for C-AST have also been previously published.^[18,20]

In this work, we tested four cell mini-module laminates (343 mm \times 370 mm with glass front-sheet, ethylene vinyl acetate (EVA) encapsulant, and a polyamide-outer layer backsheet using C-AST. The temperature was taken as the average of two thermocouples on the rear. For quantifying the humidity and to evaluate the hydrolytic degradation inside the backsheet in the Tropical sequence, digital temperature and humidity sensors were laminated internal to the functional four-cell mini-module.^[45,46] Encapsulant and backsheet properties differ, therefore, this work must be considered as a generic example. For comparison, humidity inside modules in the field was calculated based on typical meteorological year (TMY3) data.^[27] In this work, for C-AST where conditions change rapidly, 10 s measurement and integration periods were used, whereas annual weather station data from Miami, Florida with a 1 h interval data were implemented for analyzing the use condition.

An acceleration factor analysis was performed for the Tropical climate sequence of C-AST for the effects of 1) temperature and irradiance on the outer layer polymers, 2) temperature and humidity effects on degradation of PET inner layer, 3) electrochemical degradation of cell materials based on measured leakage current through the module packaging, and 4) thermomechanical fatigue based on temperature cycles.

For the High Desert sequence, temperature and irradiance effects were considered for the degradation of the outer layer polymers. Thermomechanical fatigue based on temperature cycles was also considered in the High Desert. The High Desert sequence used desiccated air input specified as less than 5% RH, so hydrolysis and conduction on the module glass were minimal such that hydrolysis of PET and electrochemical degradation processes were neglected. The Spring sequence was relatively short with more than an order of magnitude lower degradation rate because the peak module temperature is 50 °C less than that of Tropical and High Desert with half the level of irradiance. The Dead of Winter was performed at -40 °C in the dark,

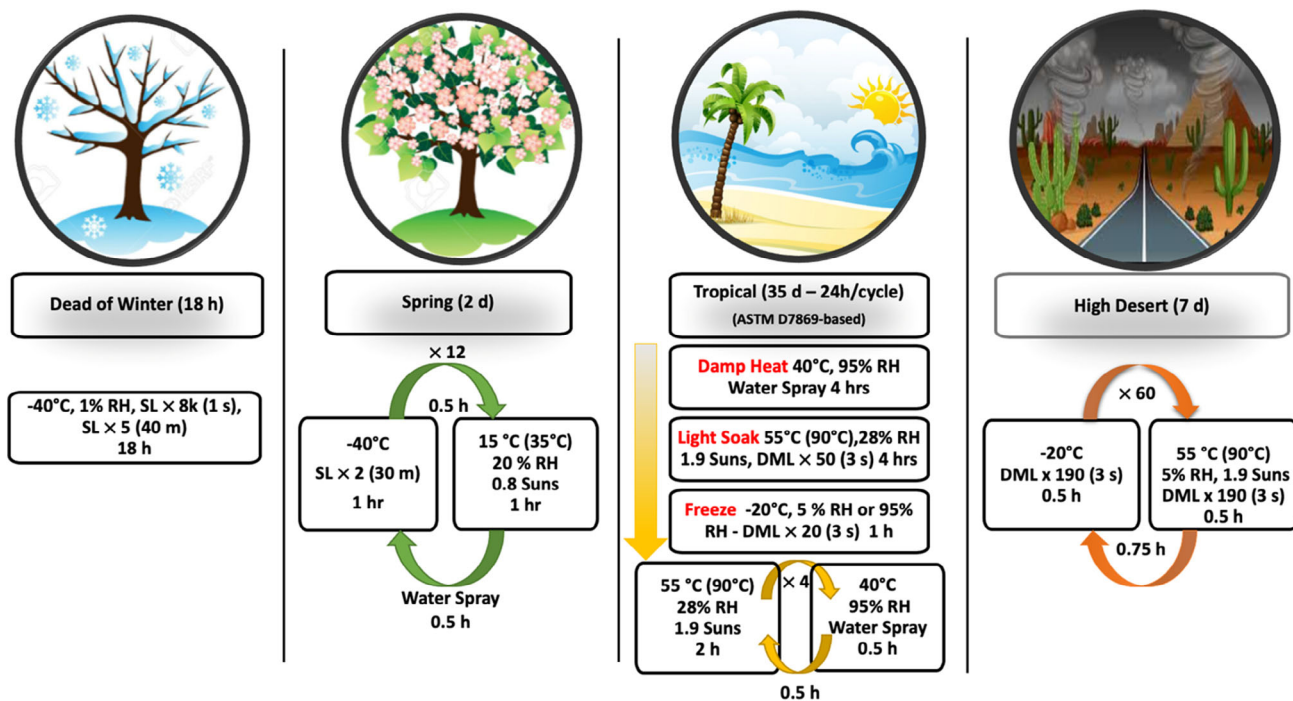


Figure 1. Illustration of the four stress sequences (climates) performed sequentially in combined-accelerated stress testing (C-AST). Undergoing the four stress sequences in the order shown is defined as one C-AST cycle. Temperatures indicated as T_{chamber} (T_{module}). -600 V system voltage is applied to cell circuit only when irradiation is applied. DML refers to cyclic dynamic loading to produce a radius of curvature that would be seen on a full-size module with 1000 Pa loading. SL is static loading with 2400 Pa equivalent. Adapted with permission.^[21] Copyright 2022, John Wiley and Sons.

so acceleration factors were not evaluated for these sequences performed at reduced temperature and irradiance.

4. Results and Discussion

Here, we show the results of the calculation and discuss the acceleration factors for various PV module degradation mechanisms for C-AST. These are hydrolysis of PET, UV degradation of outer layer polymer, electrolytic corrosion, and thermomechanical fatigue. Also discussed is cycling mechanical loading relative to windstorms for the Florida USA.

4.1. Hydrolysis of PET

Degradation of the PET layer in backsheets by hydrolysis is related to the temperature and the diffusion of moisture. **Figure 2** includes the module temperature and the module internal relative humidity that was measured by embedded sensors under the backsheet^[20,46] as well as irradiance on the module for the tropical sequence in the C-AST cycle. The damage rate as a function of temperature and relative humidity is given by Equation (3) is shown. The trends in module internal relative humidity (red line), temperature (blue line) and the resulting damage rate (lower black line-hydrolytic damage) show that during the periods when illumination by the Xe lamps is off, moisture diffuses into the module. The damage rate is the greatest when the module reaches the upper temperature (90°C), but then trends downward as moisture diffuses out under illumination with the module at the upper temperature.

For the determination of acceleration factor (Equation (6)), the denominator was calculated using TMY3 data for Miami, Florida with moisture diffusion modeling as in the study of Kempe and Wohlgemuth^[27] assuming open rack mounting and latitude tilt, and the numerator was calculated using the measured internal humidity.

$$AF_{T,RH} = \frac{\frac{1}{N_1} \sum_{N_1} (RH_{\text{chamber}})^n \cdot e^{-\frac{E_a}{k \cdot T_{\text{chamber}}}}}{\frac{1}{N_2} \sum_{N_2} (RH_{\text{outdoor}})^n \cdot e^{-\frac{E_a}{k \cdot T_{\text{outdoor}}}}} \quad (6)$$

Degradation was summed over the period of 1 year to determine $AF = f(T, RH) = 426$. The high number is associated with both the high activation energy and the exponential dependence on relative humidity. These results and those of the other calculations in this section are summarized in **Table 1**. By comparison, the acceleration of the common 85°C , 85% RH condition is on the order of 5000 using the same analysis, where 2 days at 85°C , 85% RH condition is sufficient to hydrolyze PET to the equivalent of 25 years in Miami, Florida.

4.2. UV Degradation of Outer Layer Polymer

The acceleration factor for the combined effects of temperature and UV radiation was analyzed for C-AST relative to the Miami, Florida environment. The generic rate of degradation is given in the form of Equation (4), giving the acceleration factor in C-AST as

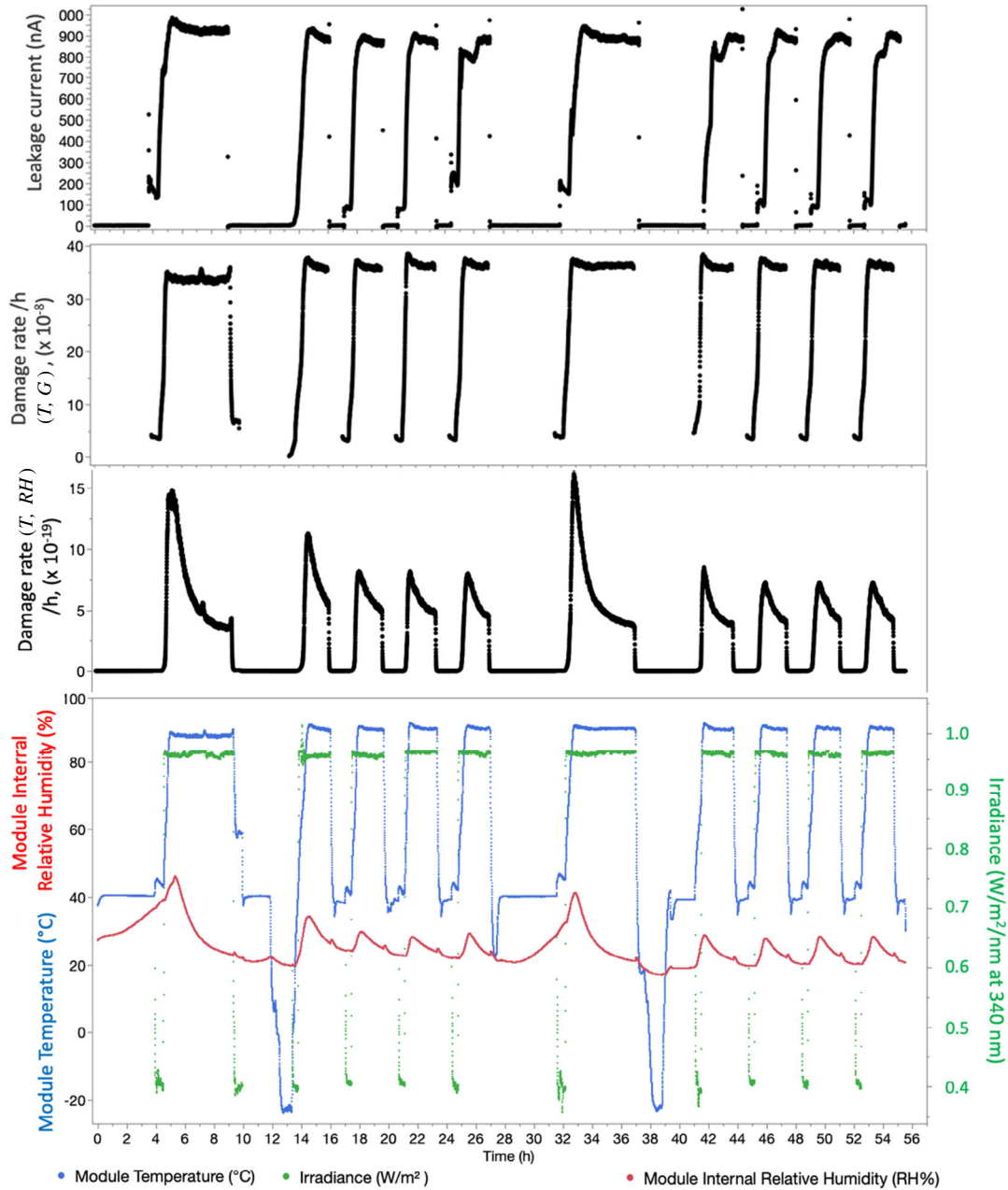


Figure 2. From top to bottom: measured leakage current from a mini-module in C-AST driving electrochemical corrosion, calculated UV damage rate of exposed polymer material, calculated hydrolytic damage rate of PET, measured stress factors (temperature, internal relative humidity, and irradiance on the module front surface) for the Tropical cycle in combined-accelerated stress testing.

$$AF_{T,G} = \frac{\frac{1}{N_1} \sum_{N_1} (G_{\text{chamber}})^x \cdot e^{-\frac{E_a}{k \cdot T_{\text{chamber}}}}}{\frac{1}{N_2} \sum_{N_2} (G_{\text{POA}})^x \cdot e^{-\frac{E_a}{k \cdot T_{\text{outdoor}}}}} \quad (7)$$

where G_{chamber} and G_{POA} are respectively the irradiance on samples in accelerated test and the plane of array of modules in the field. An acceleration of 17.3 and 10.5 compared to the Florida environment is determined for the Tropical and High Desert sequences, respectively. The higher acceleration factor with

the Tropical cycle is because of the greater proportion of time the module is at the maximum temperature (90 °C) with full irradiance (both 1.9 Suns at 340 nm).

4.3. Electrolytic Corrosion

Total coulombs transferred by application of system voltage per unit perimeter length is compared between modules in the Tropical climate sequence and in the field. The acceleration factor for electrolytic corrosion evaluated empirically by comparing

Table 1. Acceleration factors calculated for the combined-accelerated stress testing sequences (high desert and tropical) over Florida environment.

Degradation mode (stress factors) ^{a)}	Acceleration factor	
	High Desert	Tropical
Hydrolysis of PET (temperature and humidity)		426
UV degradation of out-layer polymers (temperature and irradiance)	10.5	17.3
Electrochemical degradation (voltage bias, temperature, humidity)		14.1
Fatigue of solder joints (temperature history)	28.6	23.5

^{a)}Abbreviation: PET: polyethylene terephthalate.

the current transfer over the course of 1 year is given as

$$AF_1 = \frac{\frac{1}{N_1} \sum I_{\text{chamber}} \cdot \Delta t}{\frac{1}{N_2} \sum I_{\text{outdoor}} \cdot \Delta t} \quad (8)$$

The acceleration factor was determined to be 14.1 for a module with similar voltage level of 600 V in the cell circuit. A limitation of the analysis is that C-AST modules had a pseudo frame made with conductive pressure-sensitive adhesive Al tape on the glass whereas fielded modules in Coco, Florida used for comparison had a conventional aluminum frame around the glass, which may lead to some differences in the charge transfer behavior. While charge transfer is considered to be an indicator of electrochemical degradation processes such as corrosion, it is only considered an indirect indicator of the various other PID modes due to factors such as thermal- and light-promoted recovery and the because parallel current paths through the cell metallization are not believed to cause PID-shunting and PID-polarization.

4.4. Thermomechanical Fatigue

Acceleration in thermal cycling is calculated according to the method of Bosco et al., Equation (5).^[36] The mean daily maximum cell temperature change for the High Desert and Tropical sequences is from 90 to -20°C yielding $\Delta T = 110^\circ\text{C}$ and $r(T)$ is the number of transitions per year over the temperature of $T = 56.4^\circ\text{C}$. Using TMY3 data, the extent of damage by thermomechanical fatigue over the course of a year is used to determine the acceleration factors of 23.5 and 28.6 for the Tropical and High Desert cycles as compared to Florida, as summarized in Table 1.

4.5. Cyclic Mechanical Loading

Although long-term deflection data under windstorms for fielded PV modules are lacking, we attempt to semiquantitatively compare the extent of cyclic dynamic mechanical loading in C-AST to that which would occur in windstorms. In C-AST testing, we apply a total of 53 294 dynamic mechanical load cycles over the course of implementing the four climates taking 53.5 days or 1284 h. This compares to 50 400 cycles per hour for a strong

windstorm. Therefore, one cycle spanning the four climates of a C-AST cycle approximates 1.06 h of strong windstorm with module vibrations at fundamental resonant frequency of 14 Hz as introduced above. To note, the pressure cycles in C-AST are with unidirectional pressure. Resonant frequency bidirectional loading for C-AST is in development.

4.6. Benchmarking to Field Failures

There are several examples of materials studied in C-AST that also demonstrated field failure. For example, polyamide (AAA, Isovoltaic AG) backsheets showed visible cracking around the cell interconnect ribbons after about 120 days (0.33 years), with large cracks characterized after about 184 days (0.5 years) in the Tropical cycle.^[47] In comparison, there are several reports of polyamide (nylon)-based backsheets where macrocracking is observed after 6–7 years in the field^[48–50] in climates including Nevada and Arizona (USA), and Southwest France. The FTIR signatures in the field-aged samples are more similar to that of C-AST-aged modules as opposed to direct exposure with IEC 62 788-7-2 A3 condition (65°C air temperature, 90°C black panel temperature 0.8 W m^{-2} , nm at 340 nm and 20% relative humidity).^[43] This difference is most likely due to the use of direct (greater) UV exposure of the backside as opposed to indirect in C-AST. Furthermore, the spectral distribution of UV irradiation is such that the IEC 62 788-7-2 A3 condition and the albedo from Al reflectors used in C-AST and in the natural environment will all produce different spectral distributions and damage rates. At the other extreme, thermal-oxidative degradation has been produced in AAA backsheet in accelerated testing without including any UV irradiation component.^[51,52] These are good examples of how using acceleration rates that are too high or not representative has the potential to produce different, non-field representative failure modes. Assuming failure in 6 years, the C-AST Tropical sequence empirically provides an acceleration of approximately 18 for polyamide (AAA) for the Miami environment.

PVDF backsheets, of a type that showed cracking in the field, were examined in C-AST using the multiseason sequence. After 84 days (0.23 years) in continuous Tropical cycles followed by a single cycle of the other climate types in the multiseason testing, significant cracking of the backsheet was observed. In this case, low humidity stress sequences applied after Tropical led to embrittlement of the materials that finally manifested in cracking.^[20,43,53] This compares to field failures in this PVDF material in 5–6 years in continental climates in the Americas and Asia.^[50] Assuming field failure in 5 years, the C-AST empirically provides acceleration of about 20–26 for the PVDF failure mode.

The aforementioned examples may be used to provide an estimate for the acceleration factor for C-AST aging. Rates, such as for solder fatigue, would vary depending on mounting configuration such as close roof mount versus open rack and module construction, where glass substrates lead to greater cell temperature. Regarding hydrolysis of PET, the rate of damage in C-AST is less than in the 85°C , 85% RH damp heat condition, but large compared to the terrestrial use of PV.^[27] While the C-AST tropical sequence is more realistic, the large acceleration factor would

merit caution for false positives for materials with high activation energies like PET. Regarding electrochemical degradation, the acceleration factor is determined relative to field measurements and should be representative of subtropical locations similar to Cocoa, FL. The occurrence of surface salt (ocean-side location) and particulate contamination (soiling) can facilitate charge transfer^[54] and would be expected to affect the site-specific acceleration factor. Further studies in the field to understand the extent of wind loading and resulting oscillations and displacement of modules will be beneficial to further clarify the acceleration factors for testing.

5. Summary and Conclusion

An acceleration factor analysis was performed for C-AST, focusing on the longer, higher-stress Tropical and High Desert sequences by calculation and empirical means. The Tropical sequence, by far the longest and dominating stress sequence of the four-climate C-AST protocol implemented, was calculated to provide an acceleration factor of 14.1 or greater for the four degradation modes analyzed. Despite using more realistic stress levels and combinations at the upper statistical tails of the natural environment, acceleration factors in the 400 range for processes with high activation energy can lead to false positives, but much less so than the overly stressful 85 °C 85% RH condition. While exact quantification of empirical acceleration factors between chamber and field is difficult because the exact time of appearance of the failure in the field is not certain, calculated acceleration factors appear to agree with the benchmarking to field failures.

Acknowledgements

This work was authored in part by the National Renewable Energy Laboratory, operated by Alliance for Sustainable Energy, LLC, for the U.S. Department of Energy (DOE) under Contract No. DE-AC36-08GO28308. Funding was provided as part of the Durable Modules Consortium (DuraMAT) funded by the U.S. Department of Energy, Office of Energy Efficiency and Renewable Energy, Solar Energy Technologies Office, agreement number 32509.

Conflict of Interest

The authors declare no conflict of interest.

Data Availability Statement

The data that support the findings of this study are available from the corresponding author upon reasonable request.

Keywords

accelerated testing, durability, photovoltaic modules, reliability

Received: January 30, 2023
Published online: May 4, 2023

- [1] A. R. Hoffman, E. L. Miller, DOE/JPL 1012-78/11, Jet Propulsion Laboratory, Pasadena, CA, **1978**.
- [2] S. Thayer, in *Proceedings Annual Reliability and Maintainability Symposium*, **1976**, no. NSYM: IEEE-Inst Electrical Electronics Engineers Inc, New York, NY, pp. 76–77.
- [3] A. R. Hoffman, E. L. Miller, Bias-Humidity Testing of Solar-Cell Modules, Jet Propulsion Lab., Pasadena, CA, **1978**.
- [4] J. H. Wohlgemuth, M. Conway, D. H. Meakin, in *Conf. Record of the Twenty-Eighth IEEE Photovoltaic Specialists Conf.-2000 (Cat. No. 0'CH37036)*, IEEE, Anchorage, AK **2000**, pp. 1483–1486.
- [5] J. Berghold, S. Koch, S. Pingel, S. Janke, A. Ukar, P. Grunow, T. Shioda, *Reliability of Photovoltaic Cells, Modules, Components, and Systems VIII*, International Society for Optics and Photonics **2015**, Vol. 9563, p. 95630A.
- [6] W. Luo, Y. S. Khoo, P. Hacke, V. Naumann, D. Lausch, S. P. Harvey, J. P. Singh, J. Chai, Y. Wang, A. G. Aberle, *Energy Environ. Sci.* **2017**, *10*, 43.
- [7] IEC 62804-1 Photovoltaic (PV) Modules, Test Methods for the Detection of Potential-Induced Degradation – Part 1: Crystalline Silicon, IEC, Geneva **2015**.
- [8] IEC 61215-2:2021 Terrestrial Photovoltaic (PV) Modules, Design qualification and type approval – Part 1-1: Special requirements for testing of crystalline silicon photovoltaic (PV) modules, IEC, Geneva, CH, **2021**.
- [9] F. Kersten, P. Engelhart, H.-C. Ploigt, A. Stekolnikov, T. Lindner, F. Stenzel, M. Bartzsch, A. Szpeth, K. Petter, J. Heitmann, J. W. Müller, *Sol. Energy Mater. Sol. Cells* **2015**, *142*, 83.
- [10] E. Fokuhl, T. Naeem, A. Schmid, P. Gebhardt, T. Geipel, D. Philipp, in *36th European PV Solar Energy Conf. and Exhibition*, **2019**, Vol. 36, pp. 816–821.
- [11] F. Kersten, M. Pander, M. Koentopp, M. Turek, W. Bergholz, T. Pernau, Towards a Test Standard of Light and Elevated Temperature-Induced Degradation, PV-Tech, London **2020**.
- [12] W. Gambogi, T. Felder, S. MacMaster, K. Roy-Choudhury, B. -L. Yu, K. Stika, H. Hu, N. Phillips, T. J. Trout, *2018 IEEE 7th World Conf. on Photovoltaic Energy Conversion (WCPEC) (A Joint Conf. of 45th IEEE PVSC, 28th PVSEC & 34th EU PVSEC)*, IEEE, Piscataway, NJ **2018**, pp. 1593–1596.
- [13] M. D. Kempe, T. Lockman, J. Morse, in *2019 IEEE 46th Photovoltaic Specialists Conf. (PVSC)*, IEEE, Chicago, IL **2019**, pp. 2411–2416.
- [14] IEC 61215 Terrestrial photovoltaic (PV) modules, Design Qualification and Type Approval, International Standard IEC 61215, Geneva, CH, **2005**.
- [15] IEC IS 61215-2:2021 Terrestrial Photovoltaic (PV) Modules, Design Qualification and Type Approval - Part 2: Test Procedures, International Standard IEC 61215-2:2021, Geneva, CH, **2021**.
- [16] IEC TS 63209-1 Photovoltaic Modules, Extended-Stress Testing – Part 1: Modules, Technical Specification IEC TS 63209-1:2021, Geneva, CH, **2021**.
- [17] E. Hsi, J. C. Shieh, in *2019 IEEE 46th Photovoltaic Specialists Conf. (PVSC)*, IEEE, Chicago, IL **2019**, pp. 1653–1655.
- [18] S. Spataru, P. Hacke, M. Owen-Bellini, presented at *the 7th World Conference on Photovoltaic Energy Conversion (WCPEC-7)*, IEEE, Waikoloa Village, June 2018.
- [19] D. Miller, G. Perrin, K. Terwilliger, J. Morse, C. Xiao, B. To, S. Ulicna, C.-S. Jiang, L. T. Schelhas, P. Hacke, *IEEE J. Photovoltaics* **2022**, *12*, 1341.
- [20] M. Owen-Bellini, P. Hacke, D. C. Miller, M. D. Kempe, S. Spataru, T. Tanahashi, S. Mitterhofer, M. Jankovec, M. Topič, *Prog. Photovoltaics: Res. Appl.* **2021**, *29*, 64.
- [21] P. Hacke, A. Kumar, K. Terwilliger, P. Ndione, S. Spataru, A. Pavgi, K. R. Choudhury, G. Tamizhmani, *Progress in Photovoltaics: Research and Applications*, Electronic Publication **2022**, 1–15, <https://doi.org/10.1002/pip.3636>.

- [22] K. Hartman, P. Hacke, M. Owen-Bellini, Y. Jin, M. Cummings, A. Taylor, J. Pretorius, L. Fritzemeier, *2019 IEEE 46th Photovoltaic Specialists Conf. (PVSC)*, IEEE, Chicago, IL **2019**, pp. 2243–2248.
- [23] P. Hacke, in *NREL PV Reliability Workshop*, vol. NREL/CP-5K00-74405, Lakewood, CO **2019**, pp. 198–224, <https://www.nrel.gov/docs/fy19osti/74405.pdf>.
- [24] in *Custom Market Insights*, **2022**.
- [25] G. M. Kimball, S. Yang, A. Saproo, in *2016 IEEE 43rd Photovoltaic Specialists Conf. (PVSC)*, IEEE, Portland, OR **2016**, pp. 0101–0105.
- [26] M. Koehl, M. Heck, S. Wiesmeier, *Sol. Energy Mater. Sol. Cells* **2012**, *99*, 282.
- [27] M. D. Kempe, J. H. Wohlgemuth, in *Photovoltaic Specialists Conf. (PVSC)*, *2013 IEEE 39th*, IEEE, Tampa, FL **2013**, pp. 0120–0125.
- [28] J. E. Pickett, D. J. Coyle, *Polym. Degrad. Stab.* **2013**, *98*, 1311.
- [29] W. McMahon, H. Birdsall, G. Johnson, C. Camilli, *J. Chem. Eng. Data* **1959**, *4*, 57.
- [30] A. B. M. Köhl, Y.-H. Lee, H.-S. Wu, K. P. Scott, S. Glick, P. Hacke, H. J. Koo, presented at *31st European PV Solar Energy Conf. and Exhibition*, Hamburg, Germany, September 2015, 1858–1861, <http://publica.fraunhofer.de/documents/N-366884.html>.
- [31] M. Kempe, P. Hacke, D. Holsapple, T. Lockman, J. Morse, M. Owen-Bellini, S. Hoang, T. Lance, D. Okawa, H. Ng, *SAYURI-PV Workshop*, Tsukuba, Japan **2019**.
- [32] R. Fischer, W. Ketola, in *Third Inter. Service Life Symp.*, Federation of Societies for Coatings, Sedona, AZ, February 2004, pp. 79–92.
- [33] P. Hacke, K. Terwilliger, R. Smith, S. Glick, J. Pankow, M. Kempe, S. K. I. Bennett, M. Kloos, *Photovoltaic Specialists Conf. (PVSC)*, *2011 37th IEEE*, IEEE, Seattle, WA **2011**, pp. 000814–000820.
- [34] G. Mon, L. Wen, R. Ross, D. Adent, in *18th IEEE PVSC*, Las Vegas, NV **1985**, pp. 1179–1185.
- [35] G. R. Mon, R. G. Ross, in *8th IEEE Photovoltaic Specialist Conf.*, Las Vegas, NV **1985**, pp. 1142–1149.
- [36] N. Bosco, T. J. Silverman, S. Kurtz, *Microelectron. Reliab.* **2016**, *62*, 124.
- [37] M. Assmus, S. Jack, K. A. Weiss, M. Koehl, *Prog. Photovoltaics: Res. Appl.* **2011**, *19*, 688.
- [38] H. Seigneur, E. Schneller, J. Lincoln, A. M. Gabor, in *2018 IEEE 7th World Conf. on Photovoltaic Energy Conversion (WCPEC) (A Joint Conf. of 45th IEEE PVSC, 28th PVSEC & 34th EU PVSEC)*, IEEE, Waikoloa Village Resort, HI **2018**, pp. 3810–3814.
- [39] P. Hacke, D.C. Miller, (Eds.: P. Hacke, D. C. Miller), NREL Learning, **2021**.
- [40] S.-T. Hsu, T.-C. Wu, *Energy Procedia* **2017**, *130*, 94.
- [41] M. Nichols, J. Boisseau, L. Pattison, D. Campbell, J. Quill, J. Zhang, D. Smith, K. Henderson, J. Seebergh, D. Berry, T. Misovski, C. Peters, *J. Coat. Technol. Res.* **2013**, *10*, 153.
- [42] P. Hacke, R. Smith, K. Terwilliger, G. Perrin, B. Sekulic, S. Kurtz, *Prog. Photovolt: Res. Appl.* **2014**, *22* 775.
- [43] D. C. Miller, M. Owen-Bellini, P. L. Hacke, *Sol. Energy Mater. Sol. Cells* **2019**, *201*, 110082.
- [44] S. Uličná, M. Owen-Bellini, S. L. Moffitt, A. Sinha, J. Tracy, K. Roy-Choudhury, D. C. Miller, P. Hacke, L. T. Schelhas, *Sci. Rep.* **2022**, *12*, 1.
- [45] M. Owen-Bellini, P. Hacke, M. Kempe, D. Miller, S. Spataru, L. Schelhas, S. Moffitt, presented at *the European Photovoltaic Solar Energy Conf. and Exhibition (EU PVSEC)*, Brussels, September **2018**, 1101–1105.
- [46] M. Jankovec, F. Galliano, E. Annigoni, H. Y. Li, F. Sculati-Meillaud, L.-E. Perret-Aebi, C. Ballif, M. Topic, *IEEE J. Photovoltaics* **2016**, *6*, 1152.
- [47] G. Eder, Y. Voronko, W. Muehleisen, C. Hirschl, G. Oreski, K. Knöbl, H. Sonnleitner, *IEEE PVSC 2019*, IEEE, Chicago **2019**.
- [48] J. Pascual, M. García, J. Marcos, L. Marroyo, *Prog. Photovoltaics: Res. Appl.* **2023**, *31*, 494.
- [49] W. Gambogi, S. MacMaster, B. -L. Yu, T. Felder, H. Hu, K. R. Choudhury, T. J. Trout, in *Atlas-NIST Workshop*, Gaithersburg, MD **2017**.
- [50] K. Choudhury, in *NREL Photovoltaic Reliability Workshop*, Lakewood, CO **2019**.
- [51] M. Thuis, N. M. Al Hasan, R. L. Arnold, B. King, A. Maes, D. C. Miller, J. M. Newkirk, L. T. Schelhas, A. Sinha, K. Terwilliger, S. Ulicna, K. Van Durme, *IEEE J. Photovoltaics* **2021**, *12*, 88.
- [52] P. Hacke, M. Owen-Bellini, M. Kempe, D. C. Miller, T. Tanahashi, K. Sakurai, W. J. Gambogi, J. T. Trout, T. C. Felder, K. R. Choudhury, *Advanced Micro-and Nanomaterials For Photovoltaics*, Elsevier, Amsterdam **2019**, pp. 279–313.
- [53] TR 63279:2020 Derisking photovoltaic modules, Technical Report IEC, Geneva, CH, **2020**.
- [54] P. Hacke, P. Burton, A. Hendrickson, S. Spataru, S. Glick, K. Terwilliger, in *Photovoltaic Specialist Conf. (PVSC)*, *2015 IEEE 42nd*, IEEE, New Orleans, LA **2015**, pp. 1–4.